

Kinetic study of rapidly quenched Ni₈₁P₁₉ amorphous alloys

István Virág^{a,*}, László Pöpl^a, Gábor Várhegyi^b

^aDepartment of Inorganic and Analytical Chemistry, Eötvös Loránd University, P.O. Box 32, Budapest 112, H-1518, Hungary

^bResearch Laboratory of Materials & Environmental Chemistry, Chemical Research Center, Hungarian Academy of Sciences, P.O. Box 17, Budapest, H-1525, Hungary

Received 27 July 1999; accepted 12 January 2000

Abstract

Differential scanning calorimetry (DSC) measurements with different temperature programs were used to study the crystallization kinetics of Ni₈₁P₁₉ amorphous ribbons quenched from melt at different temperatures (920–1600°C) and from a constant melt temperature (920°C) at different quenching rates leading to different thickness. A mathematical model was proposed assuming that the nuclei are formed during the preparation and pretreatment of the samples and grow during the DSC experiments. Its validity was proved by the non-linear least squares evaluation of 44 DSC experiments. This model describes our experiments better than Avrami–Erofeev equation. © 2000 Elsevier Science B.V. All rights reserved.

Keywords: NiP amorphous alloy; Crystallization kinetics; Simultaneous least-squares evaluation; DSC

1. Introduction

The structure of melted alloys has been investigated for more than 20 years [1]. Amorphous alloys can be prepared by rapid quenching from melt. The structure of the solidified amorphous alloys is determined by the liquid structure and by the relaxation processes taking place during the quenching. If there are no significant relaxation processes during the rapid quenching, then the obtained amorphous alloy keeps the internal structure of the original melt. The investigation of amorphous alloys provides valuable information on the internal structure of melting alloy, including the short- and long-range ordering. Previous Mössbauer investigations showed that the effect of relaxation on the

structure of the Ni₈₁P₁₉ alloys is much smaller than that observed in other systems [2,9].

The crystallization kinetics of the Ni₈₁P₁₉ amorphous alloy has been extensively studied [10]. The crystallization of the Ni₈₁P₁₉ alloy is an exothermal process and the differential scanning calorimetry proved to be a suitable method for investigation of the crystallization process.

In thermal analysis, the usual way of the kinetic evaluation is the application of some sort of linearization. In our opinion, these linearization techniques do not take sufficient care on the effect of experimental errors, and frequently lead to wrong results and conclusions. In other fields of chemistry the general means of kinetic evaluation is the non-linear method of least squares. Regardless of its statistical background, it is usually suitable to get an optimal or near-to-optimal fit between the measured and the theoretical data.

* Corresponding author. Tel.: +36-1-209-0555;
fax: +36-1-209-0602.
E-mail address: virag@para.chem.elte.hu (I. Virág)

Many other evaluation techniques are proposed and used in the literature of the thermal analysis, which do not involve a true, least squares curve fitting process [4,5]. In our opinion, these methods have the following drawbacks:

1. They are based on logarithmic linearization, which leads to a non-uniform sensitivity on the experimental errors.
2. Sometimes the parameter determination is based only on a few points of the experimental curves.

Therefore, the evaluations of the present work were based on the non-linear method of least squares.

2. Experimental section

2.1. Samples and preparation

The amorphous alloys of composition Ni₈₁P₁₉ were prepared by rapid quenching from melts which were treated at different temperatures (920–1600°C) for 20 min to achieve an equilibrium state. For rapid quenching we used the so-called single roller melt-spinning technique in an argon atmosphere. We had three different sample groups:

Group 1: Samples produced by different quenching rate from same temperature (950°C).

Group 2: Samples cooled down from different temperature at same quenching rate (1750 l/min).

Group 3: Samples prepared from a melt of 950°C at a 750 l/min quenching rate were subjected to a pre-annealing treatment of 0–120 min at 300°C. The pre-annealing temperature (300°C) was chosen about 40–60°C below the crystallization temperature. The heat treatments were performed in a Mettler TA-1 thermal apparatus. During the pre-annealing the samples were heated at 25–300°C/min and held for a certain time (0–120 min) before cooling to room temperature by rapid cooling rate.

2.2. Measurements and apparatus

The measurements were performed in Netzsch DSC 200 and PL 1500 DSC apparatuses in inert (argon or nitrogen) gas flow. The sample mass was about 2–3 mg. 5, 10, 15 and 20°C/min heating rates were employed to a final temperature of 600°C. A selected

sample (prepared from a melt of 950°C at a 2000 l/min quenching rate) was also studied by isothermal heating programs.

3. Applied mathematical model and evaluation method

We tried two different models in the evaluation:

1. According to the usual assumptions of the Avrami–Mampel–Erofeev model, we assumed that the nuclei form *during* the DSC experiments. The nuclei grow and later, in the ‘decay’ period of the experiments, overlap each other.
2. As an alternative description of the experiments, we assumed that the nuclei were formed *before* the DSC experiments, during the preparation and pretreatment of the samples. When the samples are heated in a DSC experiments, the nuclei start to grow and overlap each other.

The equations corresponding to the Avrami–Mampel–Erofeev model are well known [3]. We did not found, however, reliable theoretical deductions for the second case, where the nuclei form before the DSC experiments. Keeping in mind the complexity of the phenomena, we employed a formal description of the grow and overlap of the nuclei. We employed a usual, Arrhenius type equation:

$$\frac{d\alpha}{dt} = k(T)f(\alpha) \quad (1)$$

$$k(T) = A \exp\left(-\frac{E}{RT}\right) \quad (2)$$

where t is the elapsed time, T is the temperature in K, α is the fraction crystallized and $f(\alpha)$ is a function proportional to the reactive surface at a given α and A , E , and R stand for the pre-exponential factor, activation energy, and gas constant, respectively.

$f(\alpha)$ was approximated formally by the following expression [6]:

$$f(\alpha) = (\alpha + z)^m(1 - \alpha)^n \quad (3)$$

where n , m and z are parameters to be determined from the experiments. The only physical meaning of parameters m , n and z is that they together define a unique $f(\alpha)$ function. When the best values of m , n and z are found, we get an $f(\alpha)$ which approximate well the

growth and overlap of the nuclei. It is well worth to note that z cannot be 0. If z were 0, the solution of differential equation (1) would be $\alpha(t) \equiv 0$. From a physical point of view, z defines $f(0)$, which is proportional to the surface of the nuclei at the beginning of the experiments.

The calculated DSC curve, DSC^{calc} , is a linear function of $-d\alpha/dt$:

$$DSC^{\text{calc}} = -Q_0 \frac{d\alpha}{dt} \quad (4)$$

where DSC^{calc} is normalized by the initial sample mass and Q_0 is the heat of reaction in J/g. Q_0 is an unknown parameter to be determined from the experiments.

We evaluated the DSC experiments by the method of the least squares. The following least squares sum is minimized for a group of experiments evaluated together:

$$S = \sum_{i=1}^M \sum_{j=1}^{N_i} \frac{(DSC_{i,j}^{\text{exp}} - DSC_{i,j}^{\text{calc}})^2}{DSC_i^{\text{max}} M N_i} \quad (5)$$

Here $DSC_{i,j}^{\text{exp}}$ and $DSC_{i,j}^{\text{calc}}$ represent the points of a baseline-corrected DSC curve and its theoretical counterpart, respectively, in units W/g. M is the number of the experiments evaluated simultaneously. N_i is the number of experimental points in the i th experiments. DSC_i^{max} is the highest experimental value. The division by DSC_i^{max} serves to normalize S_i . The fit between the experimental and the calculated DSC curves was characterized by a deviation expressed as a percentage:

$$D = 100\sqrt{S} \quad (\%) \quad (6)$$

We minimize S to find the ‘best’ values for parameters n , m , z , E , A , Q_0 . The minimization treatment was as follows:

1. Setting initial values for the parameters.
2. Integration of differential equation (1). We used an adaptive step-size Runge–Kutta method because it proved to be an efficient integrator of Eqs. (1)–(3). The $T(t_j)$ points were connected by linear interpolation to form a continuous $T(t)$ for the adaptive step-size calculations.
3. Minimization of the least-squares sums with direct simplex search method.

FORTRAN and C++ programs were used in the evaluation with double precision arithmetic and data storage [6].

4. Results and discussion

First we evaluated the experiments by the well-known Avrami–Mampel–Erofeev model. In this way we obtained extremely high activation energy, above 2000 kJ/mol. For these reason we preferred the alternative model discussed above.

This mathematical model gave better curve fit and more reasonable parameter values than the Avrami–Erofeev equation.

4.1. Determination of parameters m and z

It is well known that the constant-heating rate experiments can be equally well described by several different $f(\alpha)$ functions. Hence we determined the parameters of $f(\alpha)$ from isothermal experiments. A sample prepared from a melt of 950°C at a 2000 l/min quenching rate was selected for these studies. The isothermal experiments were carried out at 327, 329 and 331°C, respectively.

The three isothermal experiments were evaluated simultaneously. The fit between the calculated curves is shown in Fig. 1. The parameters obtained are listed in Table 1. Parameters n , m and z were allowed to have different values in the three isothermal experiments.

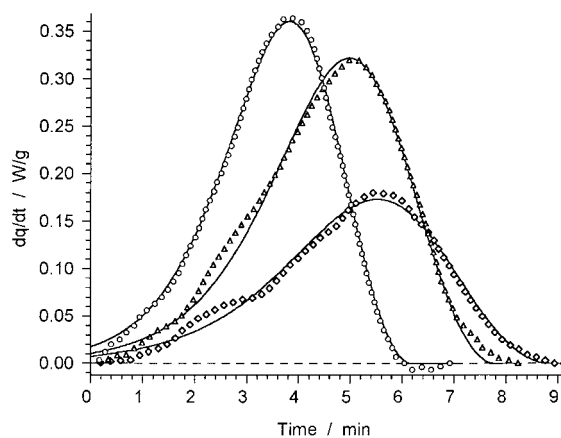


Fig. 1. The simultaneous evaluation of three isothermal DSC curves measured at 327°C (\diamond), 329°C (\triangle) and 327°C (\circ). The solid lines represent the simulated DSC curves.

Table 1

Kinetic evaluation of isothermal experiments at 327, 329 and 331°C (prepared from a melt of 950°C at a 2000 l/min quenching rate)

Temperature (°C)	E (kJ/mol)	Log A (log s ⁻¹)	n	m	z
327	245.8	19.48	0.69	1.07	6.54×10^{-4}
329	245.8	19.48	0.64	0.92	3.23×10^{-4}
331	245.8	19.48	0.66	0.95	8.44×10^{-4}
Mean	–	–	0.67	0.98	6.07×10^{-4}

Nevertheless, we observed values close to each other. The means of the n and m values, $n=0.67$ and $m=0.98$ were used in the evaluation of the non-isothermal experiments as fixed values. The values of z , however, were allowed to vary from sample to sample. Note that $z \approx f(0)$ if $m \approx 1$, hence z is characterizing the reaction surface of the nuclei at the beginning of the reaction. Therefore, the value of z depends on the preparation, pretreatment and other factors affecting the samples. Fig. 2 shows the shape of the $f(\alpha)$ function at $n=0.67$ and $m=0.98$. The $f(\alpha)$ functions corresponding to the z values of Tables 1–3 cannot be discerned in a figure of usual size. They are represented by the solid line of Fig. 2. The dashed line shows the highest z value in our work, which was observed at a pre-annealed sample (see later).

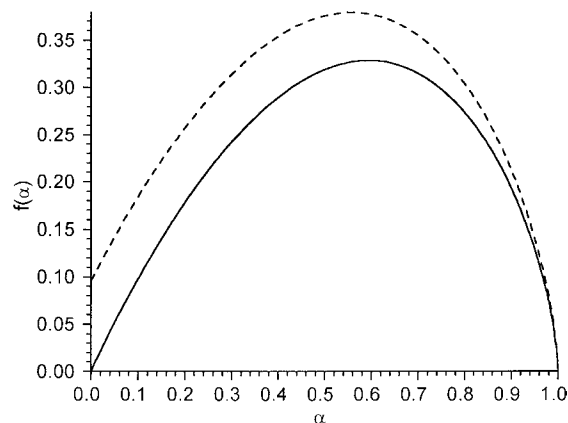


Fig. 2. The shape of the $f(\alpha)$ function at a typical z value (6×10^{-4} , —) and on the highest z value of the work (9×10^{-2} , ---).

4.2. Evaluation of the DSC curves of the Group 1 and Group 2 samples

Group 1 and Group 2 samples were studied by four DSC experiments with heating rates 5, 10, 15 and

20°C/min. The four experiments belonging to a given sample were evaluated simultaneously by the method of least squares. The results are summarized in Tables 2 and 3. The parameters clearly show the well-known

Table 2

Kinetic evaluation of alloy solutions prepared at different quenching rate (different thickness) and same melt temperature (950°C)

Quenching rate (l/min)	Thickness (μm)	E (kJ/mol)	Log A (log s ⁻¹)	z
4500	13	179.6	13.81	8.30×10^{-4}
4000	13	177.8	13.66	5.24×10^{-4}
3500	15	178.5	13.71	3.15×10^{-4}
3000	18	176.7	13.55	7.35×10^{-4}
2500	20	186.3	14.38	8.12×10^{-4}
2000	23	194.3	15.08	1.05×10^{-3}
1750	30	198.1	15.42	6.23×10^{-4}
1500	35	206.8	16.16	7.28×10^{-4}
1250	39	192.5	14.91	4.20×10^{-4}
1000	45	189.0	14.62	7.28×10^{-4}
750	65	170.9	13.16	2.79×10^{-4}
Mean	–	186.4	14.41	6.40×10^{-4}
Deviation	–	10.7	0.92	2.36×10^{-4}

Table 3

Kinetic evaluation of alloy solutions obtained from melts of different temperatures at the same quenching rate (1750 l/min)

Solution temperature (°C)	E (kJ/mol)	Log A (log s ⁻¹)	z
920	323.3	26.36	7.59×10^{-4}
1050	344.3	28.36	3.51×10^{-4}
1100	311.2	25.34	8.73×10^{-4}
1300	323.3	26.25	4.29×10^{-4}
1400	312.3	25.34	9.11×10^{-4}
Mean	322.9	26.33	6.65×10^{-4}
Deviation	13.3	1.23	2.58×10^{-4}

‘kinetic compensation effect’. In our opinion, the correlation derives from a mathematical relation between E and $\log A$ [7,8]. The scattering in Tables 2 and 3 can be due to the various experimental errors. Consequently, the means and the standard deviations of the parameters are also given in Tables 2 and 3. The highest temperature employed in the sample preparation, 1600°C resulted in a sample, which behaved entirely differently from the rest of *Group 2*. In that case the evaluation by models (1)–(4) resulted in $E=727.4$ and $\log A=60$. These unusually high values indicate that our model gives only a formal description for the 1600°C sample.

4.3. Evaluation of the DSC curves of the Group 3 samples

In *Group 3* all sample were studied by three DSC experiments with heating rates 5, 10 and 20°C/min. The three experiments belonging to a given sample

Table 4

Kinetic evaluation of samples pre-annealed at 300°C

Pre-annealing time (min)	E (kJ/mol)	Log A (log s ⁻¹)	z
0	255.5	19.57	9.29×10^{-5}
10	247.1	20.28	2.08×10^{-4}
30	238.3	18.08	7.28×10^{-4}
50	233.0	18.36	2.04×10^{-3}
70	229.9	18.79	6.70×10^{-3}
80	225.5	18.07	1.13×10^{-2}
100	222.4	17.41	3.45×10^{-2}
120	222.4	17.38	9.16×10^{-2}

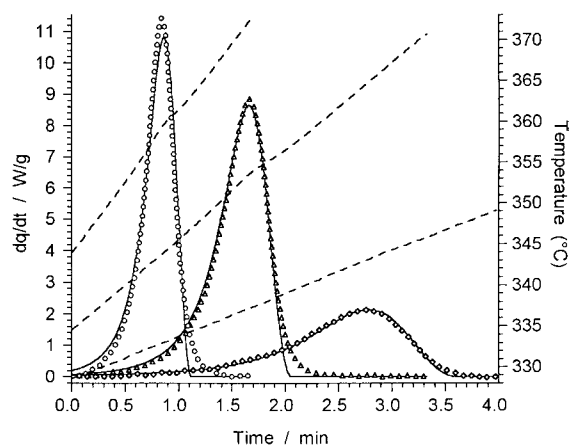


Fig. 3. Kinetic evaluation of samples prepared by 30 min pre-anneal at 300°C. From left to right: experiments at 5°C/min (○), 10°C/min (△) and 20°C/min (◇). The solid lines represent the simulated DSC curves.

were evaluated simultaneously by the method of least squares. The results are shown in Table 4 and Figs. 3–5. The data of Table 4 reveal characteristic tendencies, which are displayed in Figs. 4 and 5. $z \approx f(0)$ at $m=0.98$, hence z is characterizing the reaction surface of the nuclei at the beginning of the reaction. The increase of z shown in Fig. 4 indicates an increase of nuclei surface during the pre-anneal treatment. The accelerating rise of the curve in Fig. 4 suggests that a nucleation and the growth of nuclei take place at the temperature of the pre-annealing. E tends to 222 kJ/mol as the time of the pre-annealing

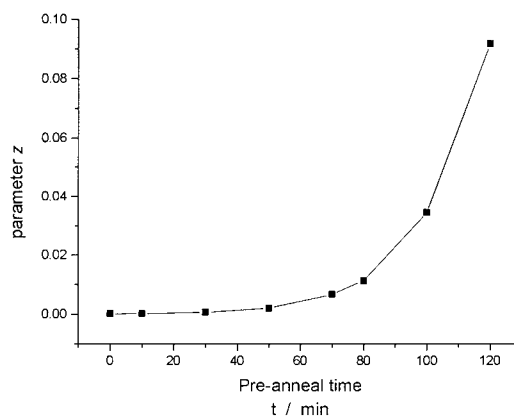


Fig. 4. The dependence of parameter z on pre-anneal time period.

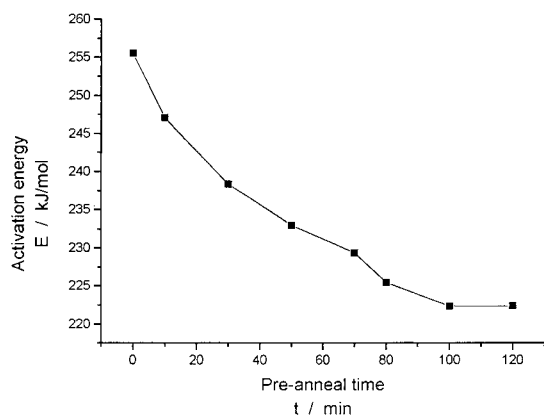


Fig. 5. The dependence of the activation energy on pre-anneal time period.

increases, which is close to the E_{growth} value reported by Lu and Wang [10].

5. Conclusions

Differential scanning calorimetry (DSC) measurements were used to study the crystallization kinetics of the $\text{Ni}_{81}\text{P}_{19}$ amorphous alloy. A mathematical model was proposed which gives better curve fit and more reasonable parameter values than the Avrami–Erofeev equation. This model assumes that the nuclei are formed before the DSC experiments, during the preparation and pretreatment of the samples. Kinetic parameters were presented for amorphous ribbons quenched from 920 to 1400°C at different quenching rate resulting in 13–65 μm thickness.

Acknowledgements

The participation of G. Várhegyi in this work was due to the help of the Hungarian National Research Fund (OTKA T 025347).

References

- [1] W. Jingtang, P. Dexing, S. Qiltong, D. Bingzhe, Effect of quenching rate on properties and structures of amorphous alloys, *Mat. Sci. Eng.* 98 (1988) 535.
- [2] E. Kuzmann, A. Cserei, A. Vértes, I.A. Novochatskii, I.A. Usatyuk, Gy. Láng, L. Kiss, F. Hajdú, L. Pöpl, Mössbauer study of phase separation in $\text{Ni}_{80}^{57}\text{Fe}_{19}$ amorphous alloys, *Hyperfine Interactions* 69 (1991) 611.
- [3] Gy. Pokol, G. Várhegyi, Kinetic aspects of thermal analysis, *Critical Rev. Anal. Chem.* 19 (1988) 65.
- [4] H.E. Kissinger, Reaction kinetics in differential thermal analysis, *Anal. Chem.* 29 (1957) 1702.
- [5] H. Schönborn, F. Haessner, Kinetics of nucleation and growth reactions investigated by DSC, *Thermochim. Acta* 86 (1985) 305.
- [6] G. Várhegyi, P. Szabó, E. Jakab, F. Till, J.-R. Richard, Mathematical modeling of char reactivity in Ar-O_2 and $\text{CO}_2\text{-O}_2$ mixtures, *Energy Fuels* 10 (1996) 1208.
- [7] M.J. Antal Jr., G. Várhegyi, E. Jakab, Cellulose pyrolysis kinetics: revisited, *Ind. Eng. Chem. Res.* 37 (1998) 1267.
- [8] G. Várhegyi, P. Szabó, M.J. Antal, Kinetics of the thermal decomposition of cellulose under the experimental conditions of thermal analysis. Theoretical extrapolations to high heating rates, *Biomass Bioenergy* 7 (1994) 69.
- [9] A. Cserei, E. Kuzmann, F. Hajdú, L. Pöpl, Gy. Láng, A. Vértes, L. Kiss, I.A. Novochatski, I.A. Usatyk, Phase analysis of $\text{Ni}_{80}^{57}\text{Fe}_{19}$ amorphous alloys solution treated at different temperatures, *Acta Chim. Hung. Acad. Sci. (Models in Chemistry)*.
- [10] K. Lu, J.T. Wang, Crystallization kinetics of Ni–P glass — activation energies for nucleation and growth of nuclei, *J. Mater. Sci.* 23 (1988) 3001.